

LOCALIZATION OF OMNI-DIRECTIONAL MOBILE DEVICE IN MULTIPATH ENVIRONMENTS

C. K. Seow and S. Y. Tan

School of Electrical and Electronic Engineering
Nanyang Technological University
Singapore 639798, Singapore

Abstract—This paper presents a comprehensive Non Line of Sight (NLOS) localization scheme in a multipath environment where the scatterers with smooth surfaces are aligned parallel or perpendicular to each other. It leverages on the estimation of Angle of Arrival (AOA) and Time of Arrival (TOA) of the omni-directional mobile device's signal received at the reference devices. Unlike the conventional Line of Sight (LOS) localization schemes that rely on the various mitigation techniques to mitigate the multipaths that are mistaken as the LOS signal, our proposed two step localization scheme not only utilizes the LOS path but also any one bound scattering NLOS multipath arriving at the reference devices for localization. Channel experiment coupled with simulation results in a typical multipath environment has demonstrated that our proposed localization scheme outperforms the conventional localization schemes that are coupled with their own mitigation techniques. Robustness in performance of our proposed localization scheme towards different scatterers' orientation where they are not aligned parallel or perpendicular to each other are also investigated.

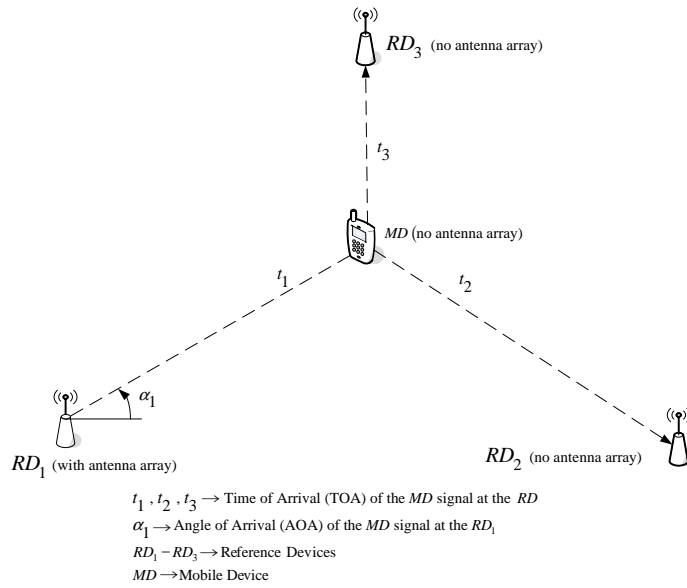
1. INTRODUCTION

There is a proliferating demand for both commercial and government applications of wireless localization services that ascertain the position of a mobile device in a cellular or sensor network [1–4]. Besides facilitating emergency safety systems to allow 911 subscriber calls, the outdoor cellular systems also accommodate proximity advertising, location sensitive billing and intelligent transport tracking systems. For the indoor channel environments, dedicated localization sensor systems have been developed that either leverage on existing indoor

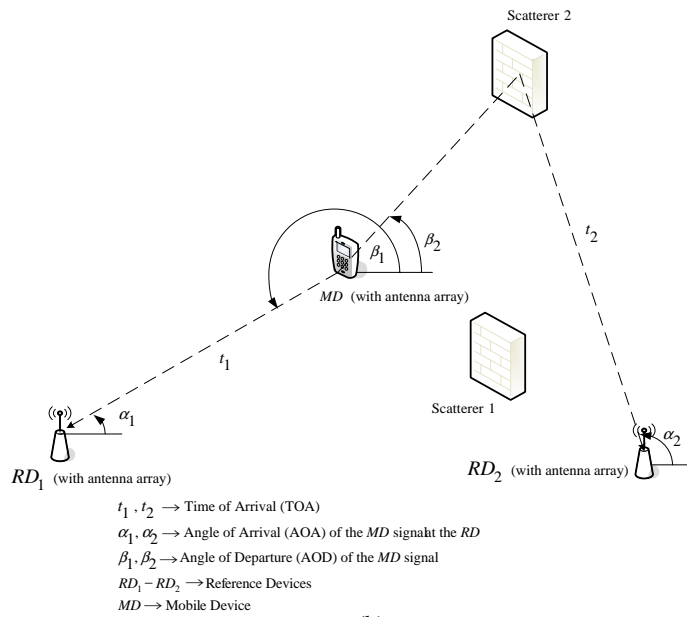
Wireless LAN 802.11x infrastructure or on specified Radio Frequency technology such as Ultra Wideband (UWB) [5–9]. These systems have been designed to provide localization information for applications such as the tracking of assets and personnel.

There is numerous number of wireless localization estimation schemes and they can be broadly classified according into whether they take a conventional LOS or the bi-directional NLOS approach. Under the LOS approach, the LOS geometric relationship between the mobile device and its reference is exploited to establish the Euclidean distance between them and to identify the physical location of the device. The information that is used to determine the location can be the measured Time of Arrival (TOA) [10–12], the Time Difference of Arrival (TDOA) [13–15], the Angle of Arrival (AOA) [16] or the Received Signal Strength (RSS) [17] of the mobile device's signal at the reference devices. There are also hybrid localization techniques that use a combination of the above metrics such as fusion of TOA and AOA data to achieve the same ends [18–20]. In the bi-directional NLOS approaches [21–24] which are the emerging novel techniques, both the TOA and AOA measurement data for either the LOS or one bound scattering (multipath that undergoes one bound scattering phenomenon) paths or both paths at both reference and mobile devices are leveraged on for location estimation. Fig. 1 depicts the above two approaches.

In general, for the conventional LOS approach, at least two reference devices are required for AOA localization scheme and three reference devices for TOA localization scheme to produce a two dimensional estimate of the mobile device under the Line of Sight (LOS) condition. However, these conventional localization schemes pose a challenge in a rich (or heavy) multipath channel environment with numerous scatterers [25–28]. In such environments, if one or more reference devices are not in the LOS range of the mobile device, the LOS localization scheme renders erroneous estimate of the mobile location. Various NLOS mitigation techniques have emerged [12, 19, 29–34] to overcome this problem. The two emerged mitigation techniques are classified as follows: the first is called residual weighting [12, 29–31]; the second is the LOS reference devices identification methodology [19, 32–34]. The first mitigation technique attempts to minimize the contribution of the NLOS multipaths, leaving the unanswered questions of about its overall mitigation technique reliability. The second methodology focuses on the identification of NLOS reference devices and discards them for localization. However, a rich multipath environment has abundant scatterers in the proximity of both the reference and mobile devices. This may result in almost all



(a)



(b)

Figure 1. (a) Conventional LOS localization schemes that use only LOS path measurement data at the reference devices. (b) NLOS localization schemes that use both LOS and one bound scattering NLOS paths' measurement data at both reference and mobile devices.

reference devices to be in NLOS region except for the one that is the closest to the mobile device. As a result, the number of devices may not be sufficient for localization. The two NLOS mitigation techniques mentioned above will not perform satisfactorily as they require that the number of LOS reference devices that are available be greater than the number of NLOS reference devices deployed in the environment.

In recent years, Multiple Input and Multiple Output (MIMO) systems have emerged as key technologies in providing high bandwidth communications services for the next generation cellular network (4G) and the wireless LAN 802.11n. MIMO exploits antenna arrays [35–46] that are coupled with smart antenna technology at both reference and mobile devices which facilitate the AOA estimation at both ends (referred to as bi-directional estimation). Localization using such principle has been explored in [21–24]. In our earlier papers [21, 22], comprehensive bi-directional least square localization schemes have been designed that are based on the TOA and AOA measurement data of the LOS [21, 22] and one bound scattering NLOS [21] paths at both the reference and mobile devices. Multiple bound scattering NLOS multipaths have been successfully rejected through the designed proximity and multipath rejection scheme [21]. Although the bi-directional approaches [21–24] with just one reference device has been able to localize the mobile device much better than the conventional LOS approach that use three reference devices in multipath environment, the cost of using antenna array at the mobile device in term of computation and physical implementation for localization is expensive.

In this paper, we will propose a novel NLOS localization scheme that removes the above mentioned limitation pertaining to the NLOS approach. It just uses the TOA and AOA measurement data of the mobile device's signal arriving at the reference devices and yet able to localize the non directional mobile device using not only the LOS path but also utilizing the one bound scattering NLOS multipath. The mobile device does not need to be equipped with antenna array (omni-directional). Furthermore, the proposed NLOS localization scheme which is a two step Determination and Selection (two step DS) scheme, is robust to the detrimental effect of the multiple bound scattering multipaths on the localization accuracy without leveraging on any mitigation or multipath rejection scheme. The proposed two step DS localization scheme comprises of determining the centroid (the likely mobile device location) among the cluster of Line of Possible Mobile Device Location (LPMD). These LPMDs are the lines that contain the possible mobile device location. They are constructed using the LOS and the one bound scattering NLOS paths' TOA and

AOA measurement data at the reference devices. The one bound scattering NLOS propagation paths arise from the specular reflection at the scatterers that are aligned parallel and perpendicular to each other. This centroid is found to be situated near the LPMDs of the LOS and one bound scattering NLOS paths. It segregates from the LPMDs of the multiple bound scattering paths. We will delve into the construction of these LPMDs in next section. The second step of the two step DS localization scheme is to find the appropriate pair of LPMDs that has the shortest Euclidean distance from the centroid and select it as the mobile device location. Another novel concept that is conceived in our proposed localization scheme is the adjustment of the TOA and the AOA measurement data of the LOS paths arriving at the reference devices so that these measurement data are close to the actual values once the centroid is determined. This renders more accurate location estimation. Section 2 will show the formulation of the proposed two step DS localization scheme while Section 3 will delve into the derivation of analytical localization error of our proposed localization scheme. Section 4 analyses the performance of our proposed scheme through the experimental and simulation results in a typical environment at the Nanyang Technological University, School of Electrical and Electronics Engineering (EEE). It has been demonstrated that our proposed two step DS localization scheme outperforms the conventional LOS localization schemes that are coupled with their own mitigation schemes in all cases. Conclusions on our research efforts are drawn in Section 5.

2. THEORY AND FORMULATION

2.1. Concept of Line of Possible Mobile Device Location (LPMD)

Consider a typical multipath environment [21,47–49] where the scatterers are smooth surfaces and are aligned parallel and perpendicular to each other as shown in Fig. 2. Three reference devices (*RDs*) were placed at RD_1 (25 m, 9 m), RD_2 (18 m, 4 m) and RD_3 (3 m, 14 m) with *MD* at (20 m, 10.8 m). The first dominant signal path arriving at each *RD* are shown. RD_1 and RD_3 are in LOS with the *MD* while RD_2 is in NLOS with the *MD*. To illustrate the concept of LPMD, consider the signal path that is arriving at RD_2 that has undergone one bound scattering (reflection) phenomenon at the scatterer $S_{2,1}$. The subscript “2” and “1” in the notation $S_{2,1}$ indicate the scatterer associated with RD_2 and the first dominant signal path received at RD_2 respectively. With the measured TOA $t_{2,1}$, AOA $\alpha_{2,1}$ of the one bound scattering signal path at RD_2 and

LOS point, MD_{LOS} . The exact location of MD can be determined by constructing another set of LPMDs (one $LPMD_v$ and one $LPMD_h$) using another signal path between RD_2 (or another reference device) and MD , and by locating the intersection of these two sets of LPMDs. For N reference devices with M paths each, the exact location of MD can be resolved using $2NM$ lines of LPMDs. This conceptual principle forms the working basis of our NLOS localization scheme. Fig. 3 illustrates the plot of the LPMDs for all the RDs each with a single dominant path with MD at (20 m, 10.8 m).

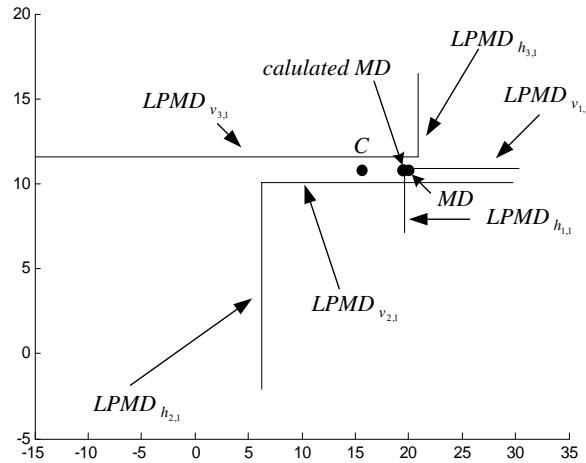


Figure 3. Plot of LPMDs for all the RDs for MD at (20 m, 10.8 m) at Nanyang Technological University, School of EEE, Block S1, Level 3 (S1-B3). The TOA standard deviation (in terms of distance) is 1 m while AOA standard deviation is 2° .

2.2. Two Step DS Localization Scheme

2.2.1. Determination of the Centriod

With reference to Figs. 2 and 3, the x axis of $LPMD_{h_{n,m}}$ and y axis of $LPMD_{v_{n,m}}$ of the RDs are utilized to determine the centriod C , which is the first estimation of the true MD location. $n = 1 \dots N$ and $m = 1 \dots M$ where N is the number of RDs and M is the number of dominant paths associated with each RD . In general, for N reference

devices with M paths each, the centroid \mathbf{C} can be found as

$$\mathbf{C} = \left[\begin{array}{c} \frac{\sum_{n=1}^N \sum_{m=1}^M w_{n,m} x_{h_{n,m}}}{\sum_{n=1}^N \sum_{m=1}^M w_{n,m}}, \frac{\sum_{n=1}^N \sum_{m=1}^M w_{n,m} y_{v_{n,m}}}{\sum_{n=1}^N \sum_{m=1}^M w_{n,m}} \end{array} \right]^T \quad (1)$$

where $x_{h_{n,m}}$ and $y_{v_{n,m}}$ are the x coordinate of the $LPMD_{h_{n,m}}$ and y coordinate of the $LPMD_{v_{n,m}}$ of the m th path of RD_n respectively. They are given as

$$x_{h_{n,m}} = x_n + d_{n,m} \cos \alpha_{n,m}, \quad y_{v_{n,m}} = y_n + d_{n,m} \sin \alpha_{n,m} \quad (2)$$

with $\mathbf{Z}_n = [x_n, y_n]^T$ as the position coordinate of RD_n and $d_{n,m} = ct_{n,m}$. $t_{n,m}$ and $\alpha_{n,m}$ are the TOA and AOA of the m th signal path of RD_n respectively. c is the speed of propagation and $w_{n,m}$ is the path weight associated with the m th path of RD_n . It is given by

$$w_{n,m} = \frac{1}{d_{n,m}^2} e^{-(\sigma_{d_{n,m}} + d_{n,m} \sigma_{\alpha_{n,m}})} \quad (3)$$

This path weight is an inverse function of the square of the propagation distance $d_{n,m}$. It can be also correlated to the power of the m th signal path at RD_n where it is inversely proportional to the square of the propagation distance $d_{n,m}$. The longer the propagation distance the path has, the lesser the weight is being assigned to this path. The rationale is that in general, the multiple bound scattering path will have longer propagation distance [21, 47–49]. By assigning lesser weight, we are able to segregate our centroid from the LPMDs of the multiple bound scattering path. $\sigma_{d_{n,m}}$, $d_{n,m} \sigma_{\alpha_{n,m}}$ are the standard deviation of TOA and AOA measurement noises (in terms of distances) respectively where $\sigma_{d_{n,m}} = c \sigma_{t_{n,m}}$. $\sigma_{t_{n,m}}$, $\sigma_{\alpha_{n,m}}$ are the actual standard deviation of TOA and AOA measurement noises respectively. Similarly, the higher the standard deviations are, the lower the weight is assigned to the associated path. Fig. 3 depicts the LPMDs of all the paths arriving at the RD s where $N = 3$, $M = 1$ for MD located at (20 m, 10.8 m) with $\sigma_{d_{n,m}} = 1$ m and $\sigma_{\alpha_{n,m}} = 2^\circ$. As shown, the centroid is estimated close to the actual MD location.

2.2.2. Selection of the Intersection Point

The next step is to determine the MD location by selecting a pair of LPMDs (a $LPMD_h$ and a $LPMD_v$) that has the smallest

Euclidean distance between the intersection point of such pair of LPMDs and the centroid \mathbf{C} . For $2NM$ number of LPMDs (one $LPMD_h$ and one $LPMD_v$ for each path), there will be $(NM)^2$ number of intersection points. The Euclidean distance between the centroid and the intersection point of a pair of LPMDs can be calculated as

$$\xi_{(h_{n,m}), (v_{j,k})} = \left\| \mathbf{C} - \mathbf{Z}_{(h_{n,m}), (v_{j,k})} \right\| \quad (4)$$

where $\mathbf{Z}_{(h_{n,m}), (v_{j,k})} = [x_{h_{n,m}}, y_{v_{j,k}}]^T$ is the intersection point of a pair of $LPMD_{h_{n,m}}$ and $LPMD_{v_{j,k}}$. $n = 1 \dots N$, $j = 1 \dots N$, $m = 1 \dots M$, $k = 1 \dots M$. Therefore the MD location $\mathbf{Z} = [x, y]^T$ can be found through the intersection point of a pair of LPMDs that has the minimum ξ and is given as

$$\mathbf{Z} = [x, y]^T = \mathbf{Z}_{(h_{n,m}), (v_{j,k}) \min \xi} = [x_{h_{n,m}}, y_{v_{j,k}}]_{\min \xi}^T \quad (5)$$

To illustrate the concept, consider Fig. 3 where $n, j = 1 \dots 3$ and $m, k = 1$. As shown in the diagram, the pair of LPMDs that has the minimum ξ is the $LPMD_h$ and $LPMD_v$ that arises both from RD_1 . As the result, the calculated MD is given as $\mathbf{Z} = \mathbf{Z}_{(h_{1,1}), (v_{1,1})} = [x_{h_{1,1}}, y_{v_{1,1}}]^T$. This is very close to the actual MD located at (20 m, 10.8 m) as shown.

2.3. LOS Path Identification and Enhancement Technique

With the calculated centroid \mathbf{C} in (1), we can obtain an estimated LOS TOA and AOA measurement data between the centroid and the reference device which is calculated as

$$r_{n,1} = \|\mathbf{C} - \mathbf{Z}_n\| \quad \beta_{n,1} = \tan^{-1} \left(\frac{[\mathbf{C}]_2 - [\mathbf{Z}_n]_2}{[\mathbf{C}]_1 - [\mathbf{Z}_n]_1} \right) \quad (6)$$

where $r_{n,1}, \beta_{n,1}$ are the calculated LOS TOA (in terms of distance) and AOA at the centroid respectively. $[\mathbf{C}]_1$ and $[\mathbf{Z}_n]_1$ are the x or first component of the column vector $[\mathbf{C}]$ and $[\mathbf{Z}_n]$ respectively. Similarly, $[\mathbf{C}]_2$ and $[\mathbf{Z}_n]_2$ are the y or second component of the column vector $[\mathbf{C}]$ and $[\mathbf{Z}_n]$ respectively. Therefore, a measurement path can be considered a LOS path if

$$|\alpha_{n,1} - \beta_{n,1}| \leq 180^\circ \pm 3\sigma_{\alpha_n} \quad |d_{n,1} - r_{n,1}| \leq 3\sigma_{d_n} \quad (7)$$

where σ_{d_n} and σ_{α_n} represent the maximum standard deviation of the TOA (in terms of distance) and AOA measurement noise at RD_n

respectively. We will use the notation that $m = 1$ is the LOS path since it is always the shortest path.

In relation to a LOS path that has been confirmed by satisfying the criteria in (7), we can ingeniously improve the accuracy of $\alpha_{n,1}$ because of the geometrical relationship [21] that exists between $\alpha_{n,1}$ and $\beta_{n,1}$ as shown in Fig. 4. As shown, $\alpha'_{n,1}$ and $\beta'_{n,1}$ has the following relationship with $\alpha_{n,1}$ and $\beta_{n,1}$

$$\alpha'_{n,1} = \alpha_{n,1}, \quad \beta'_{n,1} = 360^\circ - \beta_{n,1} \quad (8)$$

with

$$\alpha_{n,1} = \alpha_{n,1}^o + n_{\alpha_{n,1}}, \quad \beta_{n,1} = \beta_{n,1}^o + n_{\beta_{n,1}} \quad (9)$$

where $\alpha_{n,1}^o$ and $\beta_{n,1}^o$ denote the true noise free AOA values of the LOS path for RD_n and the centroid \mathbf{C} respectively. $n_{\alpha_{n,1}}$ and $n_{\beta_{n,1}}$ represent the Gaussian noise associated with each. Under ideal circumstance where the noises are absent, the following angle relationship will always hold:

$$\alpha'_{n,1} + \beta'_{n,1} = \alpha_{n,1}^o + \beta_{n,1}^o = 180^\circ \quad (10)$$

The impact of measurement noise on $\alpha_{n,1}$ and $\beta_{n,1}$ will render (10) an inequality. However, we can minimize the noise error in $\alpha_{n,1}$ and $\beta_{n,1}$ and reestablish the equality relationship by adjusting the values of $\alpha_{n,1}$ and $\beta_{n,1}$ using the following criteria:

$$e_n = \alpha'_{n,1} + \beta'_{n,1} - 180^\circ \quad (11)$$

$$\alpha'_{n,1} = \alpha'_{n,1} - e_n f_{\alpha_n}, \quad \beta'_{n,1} = \beta'_{n,1} - e_n f_{\beta_n} \quad (12)$$

where e_n is defined as the noise angle difference for RD_n and $f_{\alpha_n}, f_{\beta_n}$ are the respective error weighting factors which are calculated as

$$f_{\alpha_n} = \frac{\sigma_{\alpha_n}}{\sigma_{\alpha_n} + \sigma_{\beta_n}}, \quad f_{\beta_n} = \frac{\sigma_{\beta_n}}{\sigma_{\alpha_n} + \sigma_{\beta_n}} \quad (13)$$

σ_{β_n} is the standard deviation of the calculated AOA of the LOS path at the centroid. As for the TOA of the LOS path, the measured $d_{n,1}$ is replaced by the calculated $r_{n,1}$ in (6). Therefore by using (6), (7) and (12), the accuracy of both the measured TOA and AOA of the LOS path can be improved. By recalculating the centroid \mathbf{C} in (1) and the new intersection point ξ in (4) once again with the adjusted LOS path's TOA and AOA, the MD location accuracy is further improved.

3. ANALYTICAL PERFORMANCE BOUND

In all estimator design problems, it is important to determine the performance of the proposed estimator analytically so that we can understand the performance of the estimator at a glance without resorting to tedious simulation. One of the main criteria on the performance of the estimator is the Mean Square Error (MSE) variance of the estimator [21, 50]. In the following sections, we will derive both the LOS and NLOS path localization error variance for our two step DS localization scheme.

3.1. Proposed NLOS Path Localization Error Variance

Assume that the unidirectional measurement data $d_{n,m}$, $\alpha_{n,m}$ are independent Gaussian random variables, such that $d_{n,m} \sim N(d_{n,m}^o, \sigma_{d_{n,m}}^2)$ and $\alpha_{n,m} \sim N(\alpha_{n,m}^o, \sigma_{\alpha_{n,m}}^2)$ [18, 19, 21–24]. $d_{n,m}^o$ and $\alpha_{n,m}^o$ are the actual values of the TOA and AOA of the m th path of RD_n respectively. $\sigma_{d_{n,m}}^2$ and $\sigma_{\alpha_{n,m}}^2$ are the noise variances of the TOA and AOA of the m th path of RD_n respectively. Defining $\boldsymbol{\theta}^o = [\mathbf{d}^{oT}, \boldsymbol{\alpha}^{oT}]^T$, $\boldsymbol{\theta} = [\mathbf{d}^T, \boldsymbol{\alpha}^T]^T$ where $\mathbf{d}^o = [d_{1,1}^o \dots d_{N,M}^o]^T$, $\mathbf{d} = [d_{1,1} \dots d_{N,M}]^T$, $\boldsymbol{\alpha}^o = [\alpha_{1,1}^o \dots \alpha_{N,M}^o]^T$, $\boldsymbol{\alpha} = [\alpha_{1,1} \dots \alpha_{N,M}]^T$. We also let the variance $\boldsymbol{\sigma}_{\mathbf{d}}^2 = [\sigma_{d_{1,1}}^2 \dots \sigma_{d_{N,M}}^2]^T$ and $\boldsymbol{\sigma}_{\boldsymbol{\alpha}}^2 = [\sigma_{\alpha_{1,1}}^2 \dots \sigma_{\alpha_{N,M}}^2]^T$. For small variance of the measurement data, we can adopt the Taylor series first order expansion [50] and approximate the estimated coordinates of the MD from the minimum ξ (5) as

$$\begin{aligned} x_{h_{n,m}}(\boldsymbol{\theta}) &\approx x_{h_{n,m}}(\boldsymbol{\theta}^o) + \nabla x_{h_{n,m}}(\boldsymbol{\theta}^o)(\boldsymbol{\theta} - \boldsymbol{\theta}^o) \\ y_{v_{j,k}}(\boldsymbol{\theta}) &\approx y_{v_{j,k}}(\boldsymbol{\theta}^o) + \nabla y_{v_{j,k}}(\boldsymbol{\theta}^o)(\boldsymbol{\theta} - \boldsymbol{\theta}^o) \end{aligned} \quad (14)$$

where

$$\begin{aligned} \nabla x_{h_{n,m}}(\boldsymbol{\theta}^o) &= \frac{\partial x_{h_{n,m}}(\boldsymbol{\theta}^o)}{\partial \boldsymbol{\theta}^T} \in \Re^{1 \times 2NM} \\ \nabla y_{v_{j,k}}(\boldsymbol{\theta}^o) &= \frac{\partial y_{v_{j,k}}(\boldsymbol{\theta}^o)}{\partial \boldsymbol{\theta}^T} \in \Re^{1 \times 2NM} \end{aligned} \quad (15)$$

and subject to the constraint that

$$\xi_{(h_{n,m}), (v_{j,k})}(\boldsymbol{\theta}^o) + \sqrt{E \left[\left(\xi_{(h_{n,m}), (v_{j,k})}(\boldsymbol{\theta}) - \xi_{(h_{n,m}), (v_{j,k})}(\boldsymbol{\theta}^o) \right)^2 \right]} \quad (16)$$

is minimum. (16) is the sum of the mean and Root Mean Square (RMS) of $\xi_{(h_n,m),(v_j,k)}(\boldsymbol{\theta})$. This implies that we would always choose a set of $LPMD_h$ and $LPMD_v$ that ensures the minimum of (16) for each varying instantaneous $\boldsymbol{\theta}$ before computing (15). The $E[(\cdot)^2]$ in (16) can be derived by using Taylor series expansion as follows where

$$\xi_{(h_n,m),(v_j,k)}(\boldsymbol{\theta}) \approx \xi_{(h_n,m),(v_j,k)}(\boldsymbol{\theta}^o) + \nabla \xi_{(h_n,m),(v_j,k)}(\boldsymbol{\theta}^o) (\boldsymbol{\theta} - \boldsymbol{\theta}^o) \quad (17)$$

with

$$\nabla \xi_{(h_n,m),(v_j,k)}(\boldsymbol{\theta}^o) = \frac{\partial \xi_{(h_n,m),(v_j,k)}(\boldsymbol{\theta}^o)}{\partial \boldsymbol{\theta}^T} \in \Re^{1 \times 2NM} \quad (18)$$

However, only four elements in the row vector in (18) which correspond to the set of measurement variables that arises from an associated pair of $LPMD_h$ and $LPMD_v$ are not null. In other words,

$$\begin{aligned} & \frac{\partial \xi_{(h_n,m),(v_j,k)}(\boldsymbol{\theta}^o)}{\partial d_{n,m}}, \frac{\partial \xi_{(h_n,m),(v_j,k)}(\boldsymbol{\theta}^o)}{\partial d_{v,k}}, \\ & \frac{\partial \xi_{(h_n,m),(v_j,k)}(\boldsymbol{\theta}^o)}{\partial \alpha_{n,m}}, \frac{\partial \xi_{(h_n,m),(v_j,k)}(\boldsymbol{\theta}^o)}{\partial \alpha_{v,k}} \neq 0 \end{aligned}$$

where $d_{n,m}, d_{v,k}, \alpha_{n,m}, \alpha_{v,k}$ arise from a particular pair of $LPMD_{h_n,m}$ and $LPMD_{v_j,k}$ which generates the $\xi_{(h_n,m),(v_j,k)}(\boldsymbol{\theta}^o)$ that is in consideration. Next, by rearranging (17) and taking the square and Expectation on both sides,

$$\begin{aligned} & E \left[\left(\xi_{(h_n,m),(v_j,k)}(\boldsymbol{\theta}) - \xi_{(h_n,m),(v_j,k)}(\boldsymbol{\theta}^o) \right)^2 \right] \\ & \approx \nabla \xi_{(h_n,m),(v_j,k)}(\boldsymbol{\theta}^o) E \left[(\boldsymbol{\theta} - \boldsymbol{\theta}^o) (\boldsymbol{\theta} - \boldsymbol{\theta}^o)^T \right] \nabla \xi_{(h_n,m),(v_j,k)}^T(\boldsymbol{\theta}^o) \quad (19) \end{aligned}$$

with

$$E \left[(\boldsymbol{\theta} - \boldsymbol{\theta}^o) (\boldsymbol{\theta} - \boldsymbol{\theta}^o)^T \right] = \text{diag}(\boldsymbol{\sigma}_d^{2T}, \boldsymbol{\sigma}_\alpha^{2T}) \quad (20)$$

Similarly, rearranging (14) and taking the square and Expectation on both sides,

$$\begin{aligned}
 & E \left[\left(x_{h_{n,m}}(\boldsymbol{\theta}) - x_{h_{n,m}}(\boldsymbol{\theta}^o) \right)^2 \right] \\
 & \approx \nabla x_{h_{n,m}}(\boldsymbol{\theta}^o) E \left[(\boldsymbol{\theta} - \boldsymbol{\theta}^o) (\boldsymbol{\theta} - \boldsymbol{\theta}^o)^T \right] \nabla x_{h_{n,m}}^T(\boldsymbol{\theta}^o) \\
 & E \left[\left(y_{v_{j,k}}(\boldsymbol{\theta}) - y_{v_{j,k}}(\boldsymbol{\theta}^o) \right)^2 \right] \\
 & \approx \nabla y_{v_{j,k}}(\boldsymbol{\theta}^o) E \left[(\boldsymbol{\theta} - \boldsymbol{\theta}^o) (\boldsymbol{\theta} - \boldsymbol{\theta}^o)^T \right] \nabla y_{v_{j,k}}^T(\boldsymbol{\theta}^o)
 \end{aligned} \tag{21}$$

Finally, the variance of the localization error for our proposed NLOS localization scheme in (5) can be derived as

$$\begin{aligned}
 & E \left(\left[(x - x^o)^2 \right] \right) \\
 & \approx E \left[\left(x_{h_{n,m}}(\boldsymbol{\theta}^o) - x^o \right)^2 \right] + E \left[\left(x_{h_{n,m}}(\boldsymbol{\theta}) - x_{h_{n,m}}(\boldsymbol{\theta}^o) \right)^2 \right] \\
 & E \left(\left[(y - y^o)^2 \right] \right) \\
 & \approx E \left[\left(y_{v_{j,k}}(\boldsymbol{\theta}^o) - y^o \right)^2 \right] + E \left[\left(y_{v_{j,k}}(\boldsymbol{\theta}) - y_{v_{j,k}}(\boldsymbol{\theta}^o) \right)^2 \right]
 \end{aligned} \tag{22}$$

where $[x^o, y^o]^T$ is the true *MD* location coordinate. From (22), the RMS localization error (RMSE) for our proposed NLOS localization scheme will then be given as $\sqrt{E \left(\left[(x - x^o)^2 \right] \right) + E \left(\left[(y - y^o)^2 \right] \right)}$.

3.2. Proposed LOS Path Localization Error Variance

If there is a LOS path, the variance in (20) pertaining to the LOS path need to be altered due to the readjustment of the measurement data $t_{n,1}$ and $\alpha_{n,1}$ for the LOS path of RD_n . The modified noise error arising out of the AOA measurement has to be computed before we are able to derive the variance in the localization error in the LOS path. By substituting (9) into (8) and then (11), the noise angle difference e_n can be computed as follows:

$$e_n = \begin{cases} n_{\alpha_{n,1}} - n_{\beta_{n,1}} & \text{if } 0^\circ < \alpha_{n,1} \leq 90^\circ, 270^\circ < \alpha_{n,1} \leq 360^\circ \\ n_{\beta_{n,1}} - n_{\alpha_{n,1}} & \text{if } 90^\circ < \alpha_{n,1} \leq 180^\circ, 180^\circ < \alpha_{n,1} \leq 270^\circ \end{cases} \tag{23}$$

Putting (23) into (12) and subsequently into (8), it can be found that

$$\alpha_{n,1} = \alpha_{n,1}^o + n'_{\alpha_{n,1}}, \quad n'_{\alpha_{n,1}} = n_{\alpha_{n,1}} - (n_{\alpha_{n,1}} - n_{\beta_{n,1}}) f_{\alpha_n} \tag{24}$$

where $n'_{\alpha_{n,1}}$ is the modified noise error arising from the $\alpha_{n,1}$. From (24), it is clear that modification in (12) serves to minimize the measurement noise and seeks to provide the true AOA value of $\alpha_{n,1}^o$. Therefore, by putting (24) into (20) for the AOA of the LOS path, the new $\sigma_{\alpha_{n,1}}^2$ in (20) is given as

$$\begin{aligned} E \left[(\alpha_{n,1} - \alpha_{n,1}^o) (\alpha_{n,1} - \alpha_{n,1}^o)^T \right] &= E \left[n'_{\alpha_{n,1}} n_{\alpha_{n,1}}'^T \right] \\ &= E \left[(f_{\alpha_n} - 1)^2 n_{\alpha_{n,1}}^2 + f_{\alpha_n}^2 n_{\beta_{n,1}}^2 \right] \\ &= (f_{\alpha_n} - 1)^2 \sigma_{\alpha_{n,1}}^2 + f_{\alpha_n}^2 \sigma_{\beta_{n,1}}^2 \quad (25) \end{aligned}$$

where $\sigma_{\beta_{n,1}}^2$ can be obtained similarly from Taylor series expansion of $\beta_{n,1}(\alpha_{n,1}, d_{n,1})$ and is given as:

$$\begin{aligned} \sigma_{\beta_{n,1}}^2 &= E \left[(\beta_{n,1}(\alpha_{n,1}, d_{n,1}) - \beta_{n,1}(\alpha_{n,1}^o, d_{n,1}^o))^2 \right] \\ &\approx \nabla \beta_{n,1}(\alpha_{n,1}^o, d_{n,1}^o) \text{diag} \left(\sigma_{\alpha_{n,1}}^2, \sigma_{d_{n,1}}^2 \right) \nabla \beta_{n,1}^T(\alpha_{n,1}^o, d_{n,1}^o) \quad (26) \end{aligned}$$

with

$$\begin{aligned} \beta_{n,1}(\alpha_{n,1}, d_{n,1}) &\approx \beta_{n,1}(\alpha_{n,1}^o, d_{n,1}^o) \\ &\quad + \nabla \beta_{n,1}(\alpha_{n,1}^o, d_{n,1}^o) \text{diag}(\alpha_{n,1} - \alpha_{n,1}^o, d_{n,1} - d_{n,1}^o) \\ \nabla \beta_{n,1}(\alpha_{n,1}^o, d_{n,1}^o) &= \left[\frac{\partial \beta_{n,1}(\alpha_{n,1}^o, d_{n,1}^o)}{\partial \alpha_{n,1}}, \frac{\partial \beta_{n,1}(\alpha_{n,1}^o, d_{n,1}^o)}{\partial d_{n,1}} \right] \in \Re^{1 \times 2} \end{aligned}$$

To find out the new TOA variance of the LOS path that has undergone readjustment of the measurement data, we can adopt the same approach in which the new $\sigma_{d_{n,1}}^2$ ($= \sigma_{r_{n,1}}^2$ after LOS adjustment) can be recalculated as

$$\begin{aligned} \sigma_{r_{n,1}}^2 &= E \left[(r_{n,1}(\alpha_{n,1}, d_{n,1}) - d_{n,1}^o)^2 \right] \\ &\approx \nabla r_{n,1}(\alpha_{n,1}^o, d_{n,1}^o) \text{diag} \left(\sigma_{\alpha_{n,1}}^2, \sigma_{d_{n,1}}^2 \right) \nabla r_{n,1}^T(\alpha_{n,1}^o, d_{n,1}^o) \quad (27) \end{aligned}$$

with

$$\begin{aligned} r_{n,1}(\alpha_{n,1}, d_{n,1}) &\approx r_{n,1}(\alpha_{n,1}^o, d_{n,1}^o) \\ &\quad + \nabla r_{n,1}(\alpha_{n,1}^o, d_{n,1}^o) \text{diag}(\alpha_{n,1} - \alpha_{n,1}^o, d_{n,1} - d_{n,1}^o) \\ \nabla r_{n,1}(\alpha_{n,1}^o, d_{n,1}^o) &= \left[\frac{\partial r_{n,1}(\alpha_{n,1}^o, d_{n,1}^o)}{\partial \alpha_{n,1}}, \frac{\partial r_{n,1}(\alpha_{n,1}^o, d_{n,1}^o)}{\partial d_{n,1}} \right] \in \Re^{1 \times 2} \end{aligned}$$

Therefore, the new calculated $\sigma_{\alpha_{n,1}}^2$ in (25) and $\sigma_{d_{n,1}}^2$ in (27) for the LOS path are substituted into (20) to form the variance matrix to calculate RMS localization error.

4. EXPERIMENTAL RESULTS AND DISCUSSIONS

To evaluate the performance of our proposed localization scheme, a typical environment at Nanyang Technological University, School of Electrical and Electronic Engineering (EEE), Block S1, Level B3 (S1-B3) [21] is exploited as shown in Fig. 5. Channel measurements were taken and the measured data metrics (TOAs and AOAs) were verified accordingly to the traditional ray tracing methodology [47–49]. As mentioned earlier, the three *RDs* were located at RD_1 (25 m, 9 m), RD_2 (18 m, 4 m), RD_3 (3 m, 14 m) with the concrete walls served as the scatterers as shown in the plot. For simplicity, the dominant path ($M = 1$) are extracted from each *RD* and used for performance analysis. In total, there will be three paths from the *RDs* for each performance analysis. Fig. 5 traces the actual rays between the three *RDs* and *MD*. The following scenarios will be illustrated to examine the performance of our proposed NLOS localization scheme:

- a) Case A — all *RDs* are in LOS with *MD*;
- b) Case B — two *RDs* are in LOS with *MD*; and
- c) Case C — one *RD* is in LOS with *MD*.

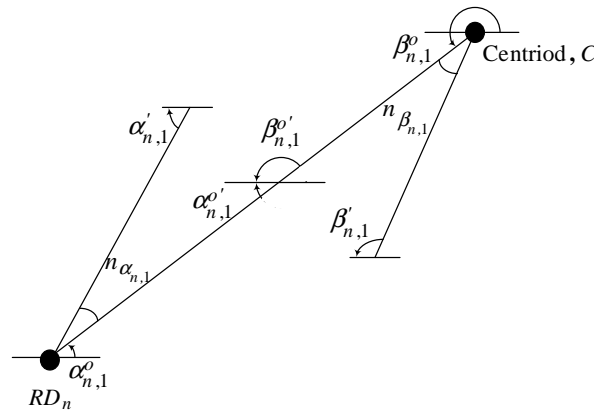


Figure 4. Geometrical relationship between AOAs for the LOS path measurement data adjustment.

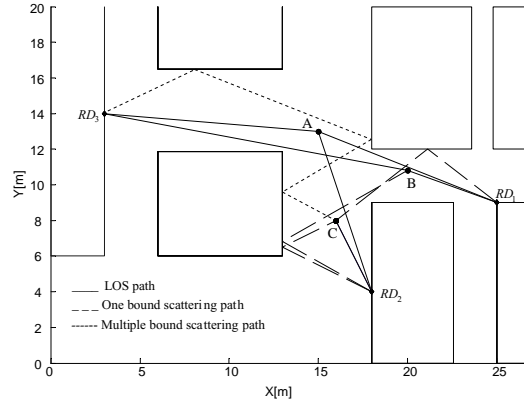


Figure 5. Ray tracing between the RDs and various MD locations at Nanyang Technological University, School of EEE, Block S1, level B3 (S1-B3).

The actual data metrics $(t_{n,m}^o, \alpha_{n,m}^o)$ are obtained by correlating ray tracing methodology with the measurement data. For thorough comparison with existing conventional localization schemes, each actual data metrics will be subjected to noise effect using Gaussian random variable noise with a mean of zero, and unknown variance (variances of all devices are identical unless otherwise specified) [18, 19, 21–24]. The RMS localization error σ_{rms} that is related to the true MD location is calculated as $\sqrt{(x - x^o)^2 + (y - y^o)^2}$. It is computed based on 10,000 independent simulation runs. MD location (x, y) is obtained from (5).

The conventional LOS localization schemes used for performance analysis are the TOA localization scheme [12], and the TOA/AOA localization scheme that is brought about by the modification of the TDOA/AOA localization scheme in [18]. The rationale for modifying [18] into TOA/AOA localization by extending the AOA formulation in [18] into TOA formulation in [12] is to allow stricter comparison. The TOA/AOA localization scheme will have lower localization error variance than the TDOA/AOA localization scheme because the latter sacrifices one time observation for the sake of synchronization. The conventional TOA localization scheme [12] has its own mitigation technique while the conventional TOA/AOA localization scheme is coupled with the LOS reference devices detection technique [19]. Furthermore as the σ_{β_n} in (13) is unknown, we equate it to σ_{α_n} which would render sufficient improvement in the LOS path measurement.

4.1. Performance Probability Distribution Due to TOA, AOA Inaccuracy

Figure 6 depicts the location accuracy of the proposed NLOS localization scheme and compares with the existing localization schemes via their cumulative probability distribution (CDF). The AOA standard deviations σ_α for all devices are 2° [21, 24, 35, 51] while the distance standard deviations σ_d are 1 m [17, 21]. In this scenario, MD is located at A (15 m, 13 m) where all RDs are in LOS with it. As shown in the plot, our proposed localization scheme's performance is equivalent to the conventional TOA/AOA localization scheme.

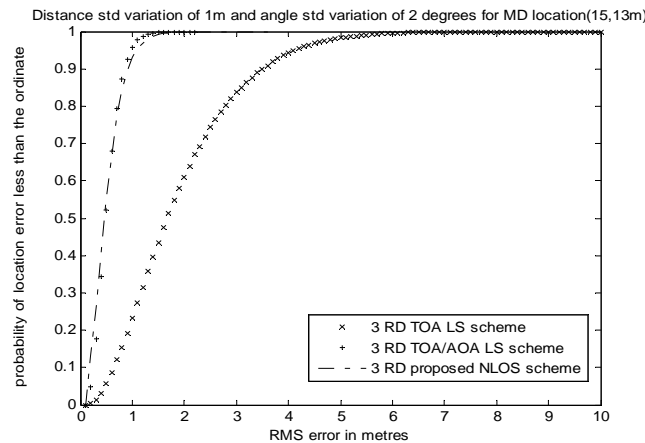


Figure 6. Comparison of the CDF performance using distance standard deviation $\sigma_d = 1$ m and AOA standard deviation $\sigma_\alpha = 2^\circ$ for MD located at (15 m, 13 m). Case A — All RDs are in LOS with MD .

Figure 7 depicts the CDF performance for MD location at B (20 m, 10.8 m). In this scenario, RD_2 is in NLOS with MD . The dominant path for RD_2 is a one bound scattering path arising out of the specular reflection at the wall (13 m, 6.83 m). Both the conventional LOS TOA and TOA/AOA localization schemes are coupled with their own NLOS mitigation schemes. For the LOS TOA/AOA localization scheme, this NLOS path is successfully detected and discarded in all the 10,000 runs. However, our proposed localization scheme still superiorly outperforms these conventional schemes, attaining $\sigma_{rms} \leq 2$ m for about 70% of the time.

Figure 8 illustrates the case where only RD_2 is in LOS with MD that is located at C (16 m, 8 m). RD_1 has a dominant one bound scattering path that arises from the specular reflection at

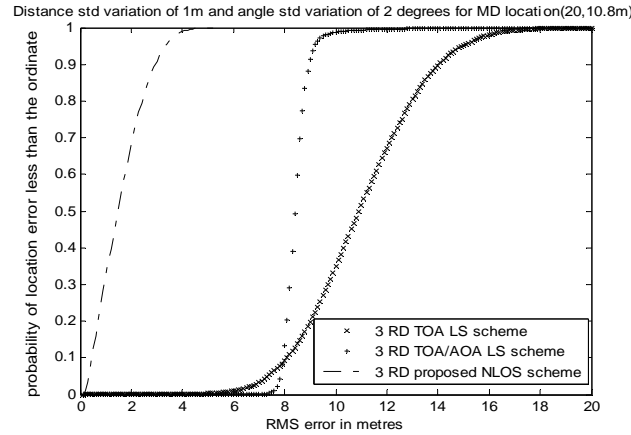


Figure 7. Comparison of the CDF performance using distance standard deviation $\sigma_d = 1$ m and AOA standard deviation $\sigma_\alpha = 2^\circ$ for *MD* located at (20 m, 10.8 m). Case B — Two *RDs* are in LOS with *MD*.

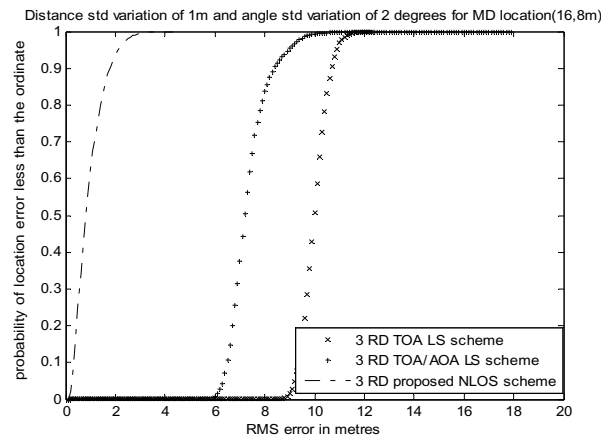


Figure 8. Comparison of the CDF performance using distance standard deviation $\sigma_d = 1$ m and AOA standard deviation $\sigma_\alpha = 2^\circ$ for *MD* located at (16 m, 8 m). Case C — One *RD* is in LOS with *MD*.

the wall (21.14 m, 12 m). For *RD*₃, the dominant path is a triple bound scattering path that undergoes three reflection at the walls (8 m, 16.5 m), (18 m, 12.5 m) and (13 m, 9.5 m). As shown, both the conventional LOS schemes' NLOS mitigation schemes could not

function well as the number of NLOS paths is greater than the number of LOS paths. As depicted, our proposed localization scheme outperforms the conventional schemes and is able to attain $\sigma_{rms} \leq 2$ m for more than 90% of the time.

4.2. Performance Bound Comparison

Figures 9 and 10 illustrate the Average Location Error (ALE) performance of all the schemes with 10,000 simulated *MD* locations. These locations are uniformly distributed in the environment to demonstrate the robustness of our proposed localization scheme. Furthermore, at these uniformly distributed *MD* locations, the dominant propagation paths arriving at the *RDs* include all possible propagation paths. These propagation paths include not only the LOS, single and multiple specular reflection paths but also single edge diffraction path and path that comprises of a combination of multiple specular reflection and a single edge diffraction. The ALE is obtained by averaging the sum of the RMS location error obtained for the 10,000 *MD* location. Fig. 9 illustrates the ALE performance for distance standard deviation of all *RDs*, $\sigma_d = 1$ m with varying AOA standard deviation, σ_α while Fig. 10 depicts the ALE performance for AOA standard deviation of all *RDs*, $\sigma_\alpha = 2^\circ$ with varying distance standard deviation, σ_d . As shown in both plots, our proposed localization scheme not only outperforms the conventional localization schemes throughout the 10,000 different *MD* locations, but also robust to the ascending AOA standard deviation. Therefore, our proposed localization scheme demonstrates performance stability in relation to variations in both the location of *MD* and the AOA standard deviation.

Figures 9 and 10 also illustrate the performance comparison between the RMS localization error of our proposed localization scheme and that of the derived analytical RMS expression (square root of the sum in (22)) for our proposed localization scheme. As shown in both plots, the difference between the analytical RMS expression and the actual localization scheme's RMS error is subtle, thus supporting the accuracy of our derived analytical expression.

4.3. Performance Due to Different Degrees of Titled Scatterer

Finally, to illustrate the robustness in performance for our proposed NLOS localization scheme in environment where some of the scatterers are not parallel or perpendicular to each other, one of the scatterers near *MD* in the environment is simulated to be titled to different

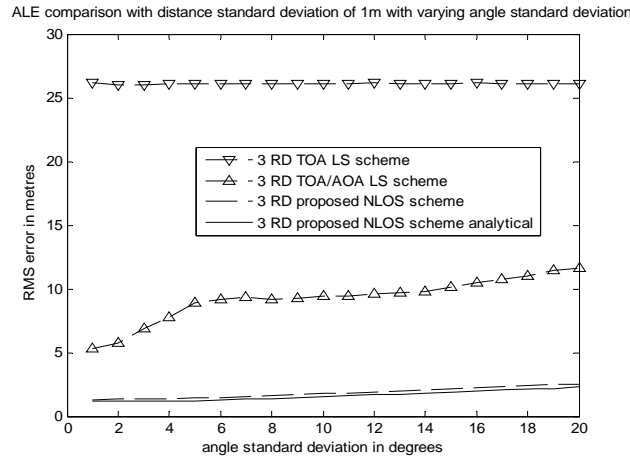


Figure 9. ALE comparison with distance standard deviation $\sigma_d = 1\text{m}$ and varying AOA standard deviation σ_α .

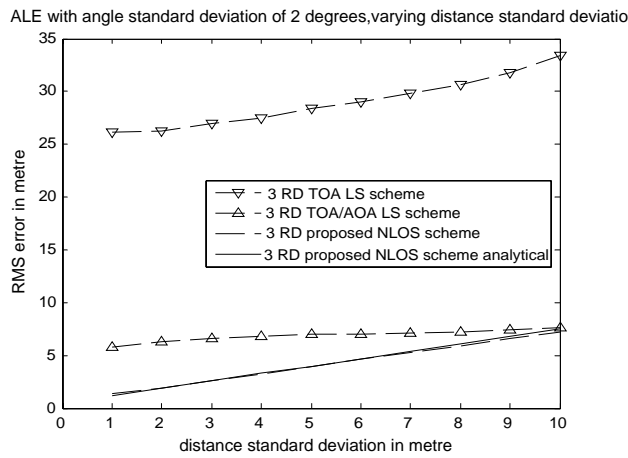


Figure 10. ALE comparison with AOA standard deviation $\sigma_\alpha = 2^\circ$ and varying distance standard deviation σ_d .

degrees, ϕ as shown in Fig. 11. The scatterer is rotated in clockwise direction at an angle ϕ from 0° to 30° . As shown, the *RDs'* received signals can transit from a LOS to a one bound scattering path as the scatterer is rotated. Fig. 12 depicts the performance of our proposed NLOS localization scheme for the titled scatterer at different degrees of clockwise rotation. As shown, our proposed localization scheme

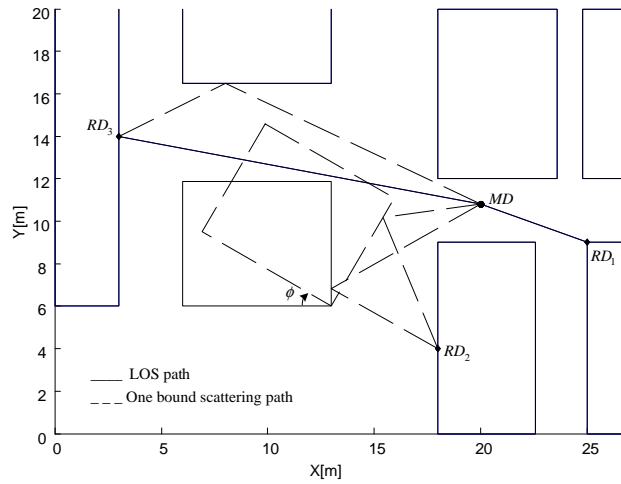


Figure 11. Ray tracing between the RDs and MD for different degrees of titled scatterer for distance standard deviation $\sigma_d = 1$ m and AOA standard deviation $\sigma_\alpha = 2^\circ$.

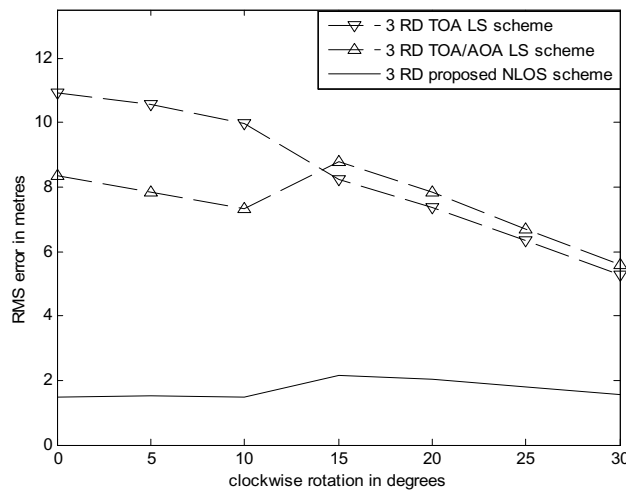


Figure 12. Performance comparison due to different degrees of titled scatterer for distance standard deviation $\sigma_d = 1$ m and AOA standard deviation $\sigma_\alpha = 2^\circ$.

still outperforms the conventional localization schemes as the titled scatterer is rotated, demonstrating our proposed scheme's performance stability in relation to variations in the scatterers' orientation and rotation.

5. CONCLUSION

A novel approach of two step NLOS localization scheme using estimation of TOA/AOA with the LOS and one bound scattering paths has been proposed with the key advantage of being able to work robustly in multipath environment. It has been demonstrated experimentally and coupled with simulations in a typical environment that our proposed NLOS localization scheme not only outperforms the conventional TOA and TOA/AOA localization schemes in all cases but also sustains performance stability in relation to variations in the location of MD , the AOA standard deviation and the scatterers' orientation. An average of $\sigma_{rms} \leq 2$ m is obtained for 90% of time for our proposed 2 step DS localization scheme without any mitigation scheme.

REFERENCES

1. Patwari, N., J. N. Ash, S. Kyperountas, A. O. Hero III, R. L. Moses, and N. S. Correal, "Locating the nodes: Cooperative localization in wireless networks," *IEEE Signal Processing Mag.*, Vol. 22, 54–69, July 2005.
2. Sayed, A. H., A. Tarighat, and N. Khajehnouri, "Network-based wireless location: Challenges faced in developing techniques for accurate wireless location information," *IEEE Signal Processing Mag.*, Vol. 22, 24–40, July 2005.
3. Reed, J. H., K. J. Krizman, B. D. Woerner, and T. S. Rappaport, "An overview of the challenges and progress in meeting the E-911 requirement for location services," *IEEE Commun. Mag.*, 30–37, Apr. 1998.
4. Yu, J. Y. and P. H. J. Chong, "An efficient clustering scheme for large and dense mobile ad hoc networks (MANETS)," *Computer Communications*, Vol. 30, 5–16, Dec. 2006.
5. Deasy, T. P. and W. G. Scanlon, "Stepwise algorithms for improving the accuracy of both deterministic and probabilistic methods in WLAN-based indoor user localization," *Int. J. Wireless Information Networks*, Vol. 11, Oct. 2004.

6. Jeong, Y.-S. and J.-H. Lee, "Estimation of time delay using conventional beamforming-based algorithm for UWB systems," *Journal of Electromagnetic Waves and Applications*, Vol. 21, No. 15, 2413–2420, 2007.
7. Soliman, M. S., T. Morimoto, and Z.-I. Kawasaki, "Three-dimensional localization system for impulsive noise sources using Ultra-wideband digital interferometer technique," *Journal of Electromagnetic Waves and Applications*, Vol. 20, No. 4, 515–530, 2006.
8. Soliman, M. S., A. Hirita, T. Morimoto, and Z.-I. Kawasaki, "Numerical and experimental study on three dimensional localization for Ultra-wideband impulsive noise sources," *Journal of Electromagnetic Waves and Applications*, Vol. 19, No. 2, 175–187, 2005.
9. Lee, J. Y. and R. A. Scholtz, "Ranging in a dense multipath environment using an UWB radio link," *IEEE J. Select. Areas Commun.*, Vol. 20, 1677–1683, Dec. 2002.
10. Liew, S. C., K. G. Tan, and C. P. Tan, "Non-Taylor series based positioning method for hybrid GPS/Cellphone system," *Journal of Electromagnetic Waves and Applications*, Vol. 20, No. 6, 717–729, 2006.
11. Chueng, K. W., H. C. So, W.-K. Ma, and Y. T. Chan, "Least square algorithms for time-of-arrival based mobile location," *IEEE Trans. Signal Processing*, Vol. 52, 1121–1128, Apr. 2004.
12. Wang, X., Z. X. Wang, and B. O. Dea, "A TOA-based location algorithm reducing the errors due to Non-Line-of-Sight (NLOS) propagation," *IEEE Trans. Veh. Tech.*, Vol. 52, 112–116, Jan. 2003.
13. Liew, S. C., K. G. Tan, and T. S. Lim, "Investigation of direct A-GPS positioning for hybrid E-OTD/GNSS," *Journal of Electromagnetic Waves and Applications*, Vol. 20, No. 1, 79–87, 2006.
14. Chan, Y. T. and K. C. Ho, "A simple and efficient estimator for hyperbolic location," *IEEE Trans. Signal Processing*, Vol. 42, 1905–1915, Aug. 1994.
15. Torrieri, D. J., "Statistical theory of passive location systems," *IEEE Trans. on Aerosp. Electron. Syts.*, Vol. 20, 183–197, Mar. 1984.
16. Alba, P. Z., V. Josep, and D. H. Brooks, "Closed form solution for positioning based on angle of arrival measurements," *Proc. IEEE Int. Symp. Personal Indoor Mobile Radio Commun. Conf.*, Vol. 14, 1522–1526, 2002.

17. Patwari, N., A. O. Hero III, M. Perkins, N. S. Correal, and R. J. O. Dea, "Relative location estimation in wireless sensor networks," *IEEE Trans. Signal Processing*, Vol. 51, 2137–2148, Aug. 2003.
18. Cong, L. and W. H. Zhuang, "Hybrid TDOA/AOA mobile users location for wideband CDMA cellular system," *IEEE Trans. Wireless Commun.*, Vol. 1, 439–447, July 2002.
19. Cong, L. and W. H. Zhuang, "Nonline-of-sight error mitigation in mobile location," *IEEE Trans. Wireless Commun.*, Vol. 4, 560–572, Mar. 2005.
20. Wang, X., P. R. P. Hoole, and E. Gunawan, "An electromagnetic-time delay method for determining the positions and velocities of mobile stations in a GSM network," *Progress In Electromagnetics Research*, PIER 23, 165–186, 1999.
21. Seow, C. K. and S. Y. Tan, "Non line of sight localization in multipath environment," *IEEE Trans. Mobile Computing*, Vol. 7, No. 5, 647–660, May 2008.
22. Seow, C. K. and S. Y. Tan, "Localisation of mobile device in multipath environment using bi-directional estimation," *IEE Electronics Letters*, Vol. 44, No. 7, 485–486, Mar. 2008.
23. Li, J., J. Connan, and S. Pierre, "Mobile terminal location for MIMO communication systems," *IEEE Trans. Antennas and Propagation*, Vol. 55, No. 8, 2417–2420, Aug. 2007.
24. Miao, H. L., K. Yu, and M. J. Juntti, "Positioning for NLOS propagation: Algorithm derivations and Cramer-Rao bounds," *Proc ICASSP 2006*, Vol. 4, 1045–1048, June 2006.
25. Jiang, L. and S. Y. Tan, "A simple analytical path loss model for urban cellular communication systems," *Journal of Electromagnetic Waves and Applications*, Vol. 18, No. 8, 1017–1032, 2004.
26. Cramer, R. J.-M., R. A. Scholtz, and M. Z. Win, "Evaluation of an ultra-wideband propagation channel," *IEEE Trans. Antennas and Propagation*, Vol. 50, 561–570, May 2002.
27. Pahlavan, K., X. R. Li, and J. P. Makela, "Indoor geolocation science and technology," *IEEE Commun. Mag.*, Vol. 40, 112–118, Feb. 2002.
28. Spencer, Q. H., B. D. Jeffs, M. A. Jensen, and A. L. Swindlehurst, "Modeling the statistical time and angle of arrival characteristics of an indoor multipath channel," *IEEE J. Select. Areas Commun.*, Vol. 18, 347–360, Mar. 2000.
29. Khajehnouri, N. and A. H. Sayed, "A non-line-of-sight

- equalization scheme for wireless cellular location,” *Proc. ICASSP 2003*, Vol. 6, 549–552, Apr. 2003.
30. Venkatraman, S., J. Caffery, Jr., and H. R. You, “Location using LOS range estimation in NLOS environments,” *Proc. IEEE Veh. Tech. Conf.*, Vol. 2, 856–860, May 2002.
 31. Chen, P. C., “A non-line-of-sight error mitigation algorithm in location estimation,” *Proc. IEEE Wireless Communications Networking Conf.*, Vol. 1, 316–320, 1999.
 32. Chan, Y. T., W. Y. Tsui, H. C. So, and P. C. Ching, “Time-of-arrival based localization under NLOS conditions,” *IEEE Trans. Veh. Tech.*, Vol. 55, 17–24, Jan. 2006.
 33. Borrás, J., P. Hatrack, and N. B. Mandayam, “Decision theoretic framework for NLOS identification,” *Proc. IEEE Veh. Tech. Conf.*, Vol. 2, 1583–1587, 1998.
 34. Xiong, L., “A selective model to suppress NLOS signals in angle of arrival (AOA) location estimation,” *Proc. IEEE Int. Symp. Personal, Indoor and Mobile Radio Commun.*, Vol. 1, 461–465, 1998.
 35. Kaiser, T., A. Bourdoux, H. Boche, J. R. Fonollosa, J. B. Anderson, and W. Utschick, “Smart antennas state of the art,” *EURASIP Book Series on Signal Processing and Communications*, Hindawi, 2005.
 36. Gershman, A. B. and N. D. Sidiropoulos, *Space Time Processing for MIMO Communications*, John Wiley & Sons, 2005.
 37. Alexiou, A. and M. Haardt, “Smart antenna technologies for future wireless systems: trends and challenges,” *IEEE Commun. Mag.*, Vol. 42, 90–97, Sep. 2004.
 38. Guo, Y. C., X. W. Shi, and L. Chen, “Retrodirective array technology,” *Progress In Electromagnetic Research B*, Vol. 5, 153–167, 2008.
 39. Hassani, H. R. and M. Jahanbakht, “Method of moment analysis of finite phase array of aperture coupled circular microstrip patch antennas,” *Progress In Electromagnetic Research B*, Vol. 4, 197–210, 2008.
 40. Zainud-Deen, S. H., H. A. Malhat, K. H. Awadalla, and E. S. El-Hadad, “Direction of arrival and state of polarization estimation using radial basis function neural network (RBFNN),” *Progress In Electromagnetic Research B*, Vol. 2, 137–150, 2008.
 41. Kazemi, S., H. R. Hassani, G. R. Dadashzadeh, and F. Geran, “Performance improvement in amplitude synthesis of unequally spaced array using least mean square method,” *Progress In*

- Electromagnetic Research B*, Vol. 1, 135–145, 2008.
42. Abdelaziz, A. A., “Improving the performance of an antenna array by using radar absorbing cover,” *Progress In Electromagnetic Research Letters*, Vol. 1, 129–138, 2008
 43. Park, G.-M. and S.-Y. Hong, “Resolution enhancement of coherence sources impinge on uniform circular array with array expansion,” *Journal of Electromagnetic Waves and Applications*, Vol. 21, No. 15, 2205–2214, 2007.
 44. Landesa, L., I. T. Castro, J. M. Taboada, and F. Obelleiro, “Bias of the maximum likelihood DOA estimation from inaccurate knowledge of the antenna array response,” *Journal of Electromagnetic Waves and Applications*, Vol. 21, No. 9, 1205–1217, 2007.
 45. Ayestaran, R. G., F. Las-Heras, and J. A. Martinez, “Non uniform-antenna array synthesis using neural networks,” *Journal of Electromagnetic Waves and Applications*, Vol. 21, No. 8, 1001–1011, 2007.
 46. Huang, M. D. and S. Y. Tan, “Spheroidal phase mode processing for antenna arrays,” *Journal of Electromagnetic Waves and Applications*, Vol. 19, No. 11, 1431–1442, 2005.
 47. Sun, Q., S. Y. Tan, and K. C. Teh, “Analytical formulae for path loss prediction in urban street grid microcellular environments,” *IEE Trans. Veh. Tech.*, Vol. 54, 1251–1258, July 2005.
 48. Tan, S. Y. and H. S. Tan, “A microcellular communications propagation model based on uniform theory of diffraction and multiple image theory,” *IEEE Trans. Antennas and Propagation*, Vol. 44, No. 10, 1317–1326, Oct. 1996.
 49. Tan, S. Y. and H. S. Tan, “Improved three-dimensional ray tracing techniques for microcellular propagation models,” *IEE Electronics Letters*, Vol. 31, 1503–1505, Aug. 1995.
 50. Kay, S. M., *Fundamentals of Statistical Signal Processing: Estimation Theory*, Vol. 1, Prentice Hall, 1993.
 51. Chandran, S., *Advances in Direction of Arrival Estimation*, Artech House Publishers, 2006.